

Quantum quench in 2D using the variational Baeriswyl wavefunction

Balázs Dóra,^{1,*} Masudul Haque,² Frank Pollmann,² and Balázs Hetényi³

¹*Department of Physics and BME-MTA Exotic Quantum Phases Research Group, Budapest University of Technology and Economics, 1521 Budapest, Hungary*

²*Max-Planck-Institut für Physik komplexer Systeme, 01187 Dresden, Germany*

³*Department of Physics, Bilkent University 06800, Ankara, Turkey*

(Dated: June 24, 2021)

By combining the Baeriswyl wavefunction with equilibrium and time-dependent variational principles, we develop a non-equilibrium formalism to study quantum quenches for two dimensional spinless fermions with nearest-neighbour hopping and repulsion. The variational ground state energy and the short time dynamics agree convincingly with the results of numerically exact simulations. We find that depending on the initial and final interaction strength, the quenched system either exhibits undamped oscillations or relaxes to a time independent steady state. The time averaged expectation value of the CDW order parameter rises sharply when crossing from the steady state regime to the oscillating regime, indicating that the system, being non-integrable, shows signs of thermalization with an effective temperature above or below the equilibrium critical temperature, respectively.

PACS numbers: 71.10.Fd,05.30.Fk,05.70.Ln

Introduction — The past decade has witnessed a massive resurgence of interest in the coherent dynamics of quantum many-body systems far from equilibrium [1–3]. This activity has been catalyzed mostly by developments in cold atom experiments [2, 4], which allow for long coherence and explicitly tracking the evolution of well-isolated many-body systems in real time. At the same time, there is also a revival of interest in the ultra-fast time evolution of solid-state systems. A ubiquitous paradigm in the theoretical study of non-equilibrium dynamics is the so-called quantum quench, where one starts from the ground state of a Hamiltonian, and then instantaneously changes a parameter, so that the system wavefunction evolves under a different Hamiltonian.

In contrast to the one-dimensional (1D) case, there are only few exact theoretical methods available to treat real-time evolution in 2D quantum systems. For example, the DMRG technique [5–11] is challenging in 2D, there are almost no 2D situations that are integrable via the Bethe ansatz, and exact numerical diagonalization is faced with a severely rapid growth of Hilbert space size. There are thus relatively few studies of interaction quenches in 2D, e.g., Refs. [12, 13] focusing mainly on short time dynamics, or Ref. [14] on time evolution in the absence of interactions.

Variational wavefunctions are vital in equilibrium condensed matter physics, e.g., the variational BCS wavefunction for superconductivity, the Yosida wavefunction for the Kondo model [15], and the Gutzwiller wavefunction (GWF) [16, 17] for the Hubbard model. The parameters of a well-chosen variational wavefunction can incorporate the most essential physics of a complex many-body system. In contrast to equilibrium, the non-equilibrium variational principle [18] has been used less extensively in correlated systems. The bosonic version of

the GWF was often used during the last decade to explore dynamics in the Bose-Hubbard model [19–21]. Recently, computational methods using Monte Carlo evaluation were formulated for the evolution of variational wavefunctions with large numbers of parameters [22–24]. In addition, the GWF within the Gutzwiller approximation [16, 17] was recently used to study the time evolution [25] of the fermionic Hubbard model. This approximation gives the exact solution of the GWF in infinite dimensions [26].

The GWF [16, 17] consists of a non-interacting wavefunction acted on by an operator which projects out states not favoured by the interaction (i.e. double occupation for the spinful Hubbard model). A completely opposite variational approach, the Baeriswyl wavefunction (BWF) [27, 28], is based on a fully localized wavefunction (an eigenfunction of the interaction term) and is acted on by a kinetic energy projector. The projector has the effect of promoting the hopping of particles in an otherwise completely localized system. In both of these approaches, the strength (coefficient) of the projection operator serves as the variational parameter.

In the present work, we will use the BWF to describe a model of 2D spinless fermions on the square lattice with nearest neighbor repulsion at half filling. The reference state is a charge density wave (CDW) with one of the sublattices exactly filled. An advantage of this approach, as we show, is that it is possible to perform the calculations exactly within the variational manifold, without the requirement of additional approximations. In addition, the wavefunction is *exact* at the two extreme limits of infinite and zero interaction. We show that equilibrium properties are well-reproduced at all interactions. We use the time-dependent variational principle [18, 29] to investigate the dynamics after interaction quenches, and show

that the system either relaxes to a steady state or oscillates indefinitely. We map out the “quantum quench phase diagram” according to this criterion and conjecture an interpretation based on the thermalization temperature. The analysis involves characteristics of the CDW order parameter. Density waves have long been a central topic in the study of electronic phases in the solid state [30]. Recent experiments have also addressed their non-equilibrium dynamics for CDW [31] as well as of related spin density (antiferromagnetic) patterns [32, 33]. The present work studies CDW dynamics for a 2D interacting system, a topic which at present lies outside the reach of exact methods.

Model — The spinless fermionic Hubbard model is defined on the 2D square lattice as $H = H_{kin} + H_{int}$ with

$$H_{kin} = -\frac{J}{2} \sum_{\langle n,m \rangle} c_n^\dagger c_m, \quad H_{int} = \frac{V}{2} \sum_{\langle n,m \rangle} n_n n_m, \quad (1)$$

where $n_n = c_n^\dagger c_n$ is the particle density operator at site n , and c_n annihilates a fermion from site n . The sum over $\langle n,m \rangle$ runs through all lattice sites and keeps only nearest-neighbor pairs. J is the strength of the single-particle hopping integral, used as the unit of energy in the following, thus it is suppressed, $V > 0$ is the strength of the nearest neighbor Coulomb repulsion. The BWF amounts to starting from the $V \rightarrow \infty$ state and using the kinetic energy as a projection operator [28]

$$|\Psi_B\rangle = N_B^{-1} \exp(\tilde{\alpha} H_{kin}) |\text{CDW}\rangle, \quad (2)$$

where $|\text{CDW}\rangle$ is the charge ordered ground state H in the atomic limit, where the charges follow a checkerboard pattern on the lattice sites (see Fig. 1), N_B is the overall normalization factor.

The BWF, due to its CDW ground state [30] possesses an appealing wavefunction in momentum space as well. The fully polarized CDW wavefunction is $|\text{CDW}\rangle = \prod_{\mathbf{k} \in \text{RBZ}} \frac{1}{\sqrt{2}} (c_{\mathbf{k}}^+ + c_{\mathbf{k}-\mathbf{Q}}^+) |0\rangle$, where $\mathbf{Q} = (\pi/a, \pi/a)$ is the ordering wavevector, a the lattice constant, the product goes through the reduced (magnetic) Brillouin zone (RBZ) and $|0\rangle$ is the fermionic vacuum. The normalized variational wavefunction assumes the form

$$|\Psi_B\rangle = \prod_{\mathbf{k} \in \text{RBZ}} \frac{\exp[\tilde{\alpha}\epsilon(\mathbf{k})]c_{\mathbf{k}}^+ + \exp[-\tilde{\alpha}\epsilon(\mathbf{k})]c_{\mathbf{k}-\mathbf{Q}}^+}{\sqrt{2 \cosh[2\text{Re}\tilde{\alpha}\epsilon(\mathbf{k})]}} |0\rangle \quad (3)$$

with $\epsilon(\mathbf{k}) = -\cos(k_x a) - \cos(k_y a)$. Here, $\tilde{\alpha} = \alpha + i\eta$ is the complex variational parameter. Its imaginary part becomes relevant when studying the quench problem.

Equilibrium properties — The variational problem is solved by minimizing the ground state energy with respect to the variational parameter $\tilde{\alpha}$ as $E_0 = \min_{\tilde{\alpha}} \langle \Psi_B | H | \Psi_B \rangle$, and our conventions imply that negative real values of $\tilde{\alpha}$ minimize the above functional, namely

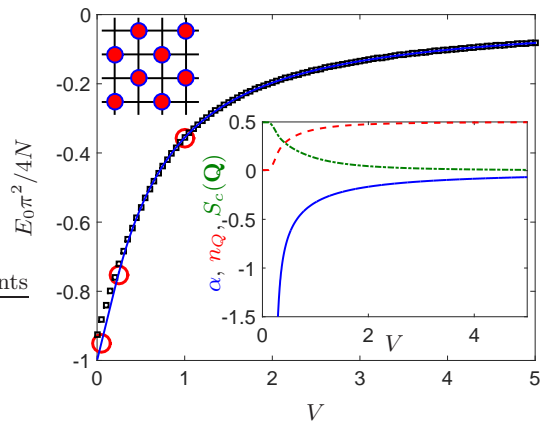


FIG. 1. (Color online) The variational ground state energy, normalized by its non-interacting value (blue solid line), is compared to 2D DMRG data (red circles) and ED on 4×4 cluster (black squares). The lower inset visualizes the CDW order parameter n_Q (red dashed line), the equal time structure factor from Eq. (7) for momentum \mathbf{Q} (green dash-dotted line) and the variational parameter, α (blue solid line) as a function of the interaction strength. The upper inset depicts a small segment of the fully polarized CDW state.

$\alpha < 0$ and $\eta = 0$. The expectation value of the kinetic and interaction energy is evaluated *exactly* with the variational wavefunction as $\langle H_{kin} \rangle = \epsilon(\mathbf{0}) I_2$ and

$$\langle H_{int} \rangle = -NV \frac{\epsilon(\mathbf{0})}{4} + \frac{V\epsilon(\mathbf{0})}{N} \sum_{i=1,2,3} I_i^2, \quad (4)$$

where N is the total number of lattice sites and [34]

$$I_1 = \sum_{\mathbf{k}} \frac{\cos[2\eta\epsilon(\mathbf{k})]}{2 \cosh[2\alpha\epsilon(\mathbf{k})]}, \quad (5a)$$

$$I_2 = \sum_{\mathbf{k}} \frac{\cos(k_x a)}{2} \tanh[2\alpha\epsilon(\mathbf{k})], \quad (5b)$$

$$I_3 = \sum_{\mathbf{k}} \frac{\cos(k_x a) \sin[2\eta\epsilon(\mathbf{k})]}{2 \cosh[2\alpha\epsilon(\mathbf{k})]}. \quad (5c)$$

Note that we obtain an exact, closed expression for the variational energy, $\langle H_{kin} \rangle + \langle H_{int} \rangle$ in 2D for this model. So far, closed expressions have not been derived based on the GWF for any two-dimensional model. Moreover, the energy expectation values are valid also for hypercubic lattices in arbitrary dimension d , after making the replacement $\epsilon(\mathbf{k}) = -\sum_{i=1}^d \cos(k_i a)$, and the \mathbf{k} sums run over d wavevector components.

The occupation number of momentum states is $n_{\mathbf{k}} = \langle c_{\mathbf{k}}^\dagger c_{\mathbf{k}} \rangle = 1/\{1 + \exp[-4\alpha\epsilon(\mathbf{k})]\}$. This expression corresponds to the occupation number of a non-interacting system at finite temperature with $T = -1/4\alpha$. In the following we will make use of this interpretation. The initial CDW state thus possesses infinite temperature with $n_{\mathbf{k}} = 1/2$, as follows from $|\text{CDW}\rangle$ as well, albeit it differs

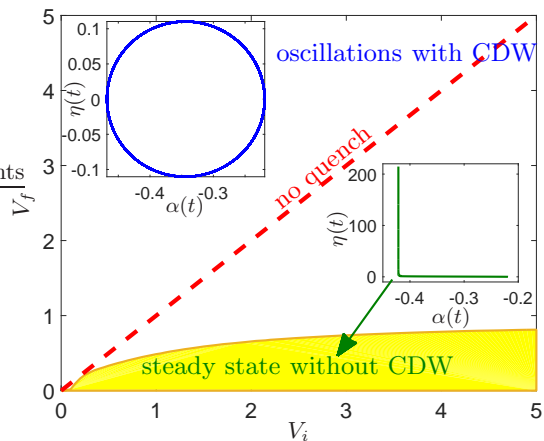


FIG. 2. (Color online) The quantum quench phase diagram for V_i and V_f is shown. For small V_f , a time independent steady state is reached which could be interpreted as an indicator thermalization at an effective temperature higher than the equilibrium CDW transition temperature with $\eta(t \rightarrow \infty) \sim t$ and $\alpha(t)$ saturating to a finite value, as depicted in the lower inset for $V_i = 1.5$, $V_f = 0.25$ and $0 < t < 200$. For sizable quenches, on the other hand, the system periodically returns to its initial state, visualized in the upper inset for $V_i = 1.5$, $V_f = 1$. For $V_i = \infty$, the transition from the steady state to oscillating behaviour occurs at $V_f \approx 0.97$.

from a trivial $T = \infty$ state due to the anomalous correlations with wavevector \mathbf{Q} from the CDW. The charge density at lattice site \mathbf{R} is

$$n(\mathbf{R}) = \frac{1}{2} + n_Q \cos(\mathbf{Q}\mathbf{R}), \quad n_Q = \frac{I_1}{N}, \quad (6)$$

with n_Q the CDW order parameter, describing the \mathbf{Q} periodic charge oscillations.

The \mathbf{Q} th Fourier component of the equal-time connected structure factor (SF), which measures non-local properties and CDW correlations, is

$$S_c(\mathbf{Q}) = \langle \Psi_B | \rho_{\mathbf{Q}} \rho_{-\mathbf{Q}} | \Psi_B \rangle - N |n_Q|^2 = \frac{1}{2} - \frac{1}{2N} \sum_{\mathbf{k}} \frac{\cos^2[2\eta\epsilon(\mathbf{k})]}{\cosh^2[2\alpha\epsilon(\mathbf{k})]}, \quad (7)$$

where $\rho_{\mathbf{Q}} = \frac{1}{\sqrt{N}} \sum_{\mathbf{k}} c_{\mathbf{k}}^+ c_{\mathbf{k}-\mathbf{Q}}$, and gives 0 in the fully polarized CDW state and 1/2 in the absence of CDW correlations, corresponding to infinite and zero effective temperatures. Therefore, the value of the SF is related to the amount of CDW order and its effective temperature of the system. It is time independent in equilibrium, shown in Fig. 1, and reflects the behaviour of n_Q .

The variational wavefunction is exact in two opposite limits, $V = 0$ ($\alpha = -\infty$) and $V = \infty$ ($\alpha = 0$). In the former case, the ground state energy is $E_0 = -4N/\pi^2$, while for the latter, the kinetic energy is suppressed by the CDW and the interaction energy reaches its minimum, therefore $E_0 = 0$. In between these two extrema,

the ground state energy, the CDW order parameter n_Q and the optimal variational parameter are shown in Fig. 1, together with numerical data using 2D DMRG and exact diagonalization (ED) on 4×4 cluster. The 2D DMRG data is obtained by extrapolating the energies for infinitely long cylinders with circumferences $L = 6, 8, 10$ to the thermodynamic limit. The agreement between the variational and numerically obtained energies is remarkable. The ED matches the DMRG data for larger V , indicating short correlation length, such that the relatively small system size does not influence the ground state energy.

The system is always in a CDW state, except for $\alpha \rightarrow -\infty$, corresponding to the non-interacting limit $V = 0$. This is in agreement with what is expected for the spinless Hubbard model on the square lattice [35, 36]. The CDW phase appears because of the square shaped Fermi surface at half filling, in the case of perfect nesting [30], and also due to the log-divergent density of states upon approaching half filling as $\sim \ln(1/\omega)$.

Quantum quench — We now turn to the investigation of the quantum quench, when an initial V_i is changed suddenly to V_f at $t = 0$. The time-dependent wavefunction is of Baeriswyl form, $|\Psi_B(t)\rangle$ as well, and the quench amounts to allowing for time-dependent variational parameters $\alpha(t)$ and $\eta(t)$ in Eq. (3). Their time-dependence follows from the time-dependent variational principle, which requires the minimization of the real Lagrangian, defined as [18, 29]

$$L(t) = -\text{Im}(\langle \Psi_B | \partial_t \Psi_B \rangle) - \langle \Psi_B | H | \Psi_B \rangle, \quad (8)$$

with respect to the time-dependent variational parameters. Using $L(t) = \langle H_{kin} \rangle (\partial_t \eta - 1) - \langle H_{int} \rangle$ with the expectation values taken from Eq. (4) with the time-dependent variational parameters, we finally arrive to the Euler-Lagrange equations, determining the quench dynamics as

$$\partial_t \alpha = \frac{\partial \langle H_{int} \rangle}{\partial \eta}, \quad \partial_t \eta = 1 + \frac{\partial \langle H_{int} \rangle}{\partial \alpha}, \quad (9)$$

supplemented with the initial conditions $\alpha(0) = \alpha_i$, originating from the equilibrium configuration for V_i , and $\eta(0) = 0$. From these, the total energy is conserved after the quench, as expected.

From Eq. (9), the two limiting cases are recovered. First, when no quench was performed, $\alpha(t) = \alpha_i$ and $\eta(t) = 0$. Second, in the case of quenching from $V_i = \infty$ to $V_f = 0$, the $\alpha_i = 0$ initial condition fixes $\alpha(t) = 0$, while $\eta(t) = t$. For general values of initial and final interactions, one needs to integrate these coupled differential equations numerically [34]. The obtained phase diagram is shown in Fig. 2. Eq. (1) in 2D is non-integrable, therefore it is expected to thermalize after a sudden quench,

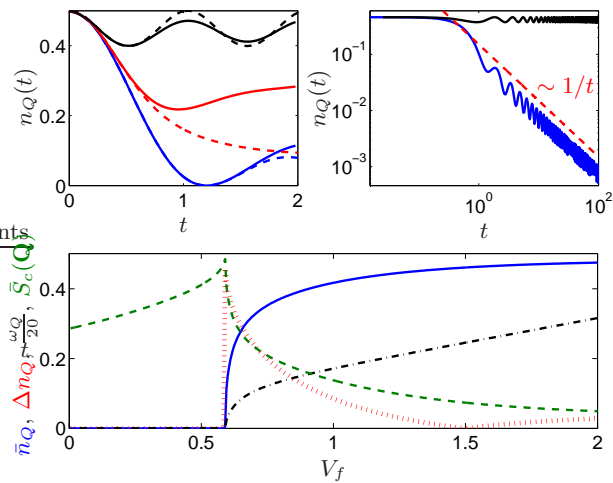


FIG. 3. (Color online) Top left: The short time decay of the CDW order parameter from time-dependent 2D DMRG for an infinite cylinder of circumference $L = 8$ (solid lines) and variational calculation (dashed lines) for $V_i = \infty$ and $V_f = 0$ (blue), 1 (red) and 2 (black). Top right: The typical behaviour of the CDW order parameter is plotted in the steady state region (blue line), vanishing as $1/t$, for $V_i = 1.5$ and $V_f = 0.25$ and in the oscillatory region (black line) for $V_i = 1.5$ and $V_f = 1$. Bottom: The time average value of the CDW order parameter (blue solid line), the amplitude (red dotted line) and the frequency (black dash-dotted line) of oscillations, together with the structure factor for momentum \mathbf{Q} (green dashed line) are shown for $V_i = 1.5$.

and we argue that our simple variational scheme is able to capture some of its physics.

The time dependence of the CDW order parameter is calculated from Eq. (6) after inserting the time-dependent variational parameters into I_1 . The short time behaviour from the BWF agrees well with that from 2D time-dependent DMRG obtained using the algorithm introduced in Ref. [11], as shown in Fig. 3. The $V_i = \infty \rightarrow V_f = 0$ quench is exact within the variational framework, which also allows us to check the temporal validity of the numerics.

For longer times, the variational solution either oscillates around its time average, or reaches a steady state after the quench [34]. For quenches with small V_f , a time independent steady state is reached with $\eta(t)$ increasing linearly with time and $\alpha(t)$ saturating to a fixed value. This can be thought of as the heating up of the system, such that it eventually thermalizes to a higher effective temperature than the equilibrium CDW transition temperature, thus CDW is absent. The CDW order parameter decays to zero since due to $\eta(t) \sim t$, the numerator in I_1 oscillates fast and kills the integral with increasing t . In particular, for arbitrary spatial dimension d , a $n_Q(t) \sim t^{-d/2}$ decay is found, in accord with special quenches of the 1D Heisenberg chain [37]. A similar decay is found for the antiferromagnetic order of the 2D spinful Hubbard model [14], quenched to a non-interacting sys-

tem. While in 1D, the CDW order parameter oscillates and changes also sign after the quench [14, 37], it only oscillates around its envelope function in 2D but does not change sign, as shown in Fig. 3. This is supported by the exact result when quenching from $V_i = \infty$ to $V_f = 0$, $n_Q(t) = J_0^d(2t)/2$, valid in arbitrary dimension d , and $J_0(x)$ is the zeroth Bessel function of the first kind, in agreement with our numerical findings.

For larger V_f , on the other hand, an oscillating solution is found for both $\alpha(t)$ and $\eta(t)$, and the system periodically returns to its initial state, and seemingly does to reach a time independent steady state, illustrated in Fig. 2. Within our approach, we interpret this as an indicator of thermalization to a thermal state with lower effective temperature than the equilibrium CDW transition temperature, hence the resulting state possesses a finite CDW order. The oscillations are artifacts of the variational calculations, but the value it oscillates around could correspond to that in the thermalized state. Throughout the time evolution, $\alpha(t)$ stays negative, and its equilibrium interpretation as an effective temperature through the momentum distribution remains true after the quench, with a time-dependent effective temperature $T(t) = -1/4\alpha(t)$.

In order to further characterize the CDW phase, we consider the time average of the order parameter as $\bar{n}_Q = \lim_{t \rightarrow \infty} \frac{1}{t} \int_0^t n_Q(t') dt'$, together with the amplitude, Δn_Q and frequency, ω_Q of the oscillations of $n_Q(t)$ in the oscillating regime, shown in Fig. 3 for the representative case of $V_i = 1.5$. Here, $\Delta n_Q = \lim_{t \rightarrow \infty} \{\max[n_Q(t)] - \min[n_Q(t)]\}$ in the oscillating regime and ω_Q is the basic harmonics of the oscillations in $n_Q(t)$, evaluated from Fourier analysis. Due to the non-integrability of the model, the system is expected to thermalize [2]. For small V_f , the CDW gap and transition temperature is small and the effective temperature, the system reaches, is above the equilibrium CDW transition temperature, therefore the CDW order is absent in this case, as evidenced in Fig. 3. For larger final interaction, however, the corresponding equilibrium transition temperature increases, and becomes equal to the effective temperature of the thermalized system, which marks the sharp rise of \bar{n}_Q . From that point on, with increasing V_f , the system's effective temperature is always smaller than the equilibrium transition temperature, therefore the system exhibits long range CDW order, mimicking a thermalized state. This scenario is further corroborated by focusing on other characteristics of the order, such as the amplitude and frequency of the oscillations in the oscillating regime.

The equal time \mathbf{Q} th structure factor after the quench is obtained by inserting the time-dependent variational parameters in Eq. (7). Its long time average, $\bar{S}_c(\mathbf{Q})$ is plotted in Fig. 3. At the critical V_f , where the transition occurs, the variational wavefunction is almost metallic, and contains enhanced CDW correlations away from this

point. However, only strong interaction can profit from these correlations and drive the dynamical CDW transition. The effective temperature after the quench is expected to increase monotonically with $|V_f - V_i|$, while the equilibrium CDW gap grows with V_f . When these two energy scales become comparable, the dynamical phase transition occurs..

Conclusion — We have studied quantum quenches for 2D spinless fermions on the square lattice with nearest-neighbour hopping and repulsion using the variational BWF, which are unaccessible by exact methods. Depending on the initial and final interaction strength, the system reaches either a time independent steady state or oscillates periodically in time. We argue by investigating the characteristics of the CDW order parameter and the equal time structure factor that the former and latter behave similarly to what is expected from a thermal state with effective temperature larger and smaller than the equilibrium CDW transition temperature, respectively.

Our work opens up a number of interesting questions worth pursuing in the future, such as considering bosons instead of fermions, the effect of disorder, the influence of imperfect nesting, incorporating the spin degree of freedom, as well as the improvement of the variational method by introducing variational parameters for each \mathbf{k} mode.

We thank Johannes Motruk for sharing 2D DMRG data for the equilibrium case. BD was supported by the Hungarian Scientific Research Funds Nos. K101244, K105149, K108676 and by the Bolyai Program of the HAS. BH was supported by the Turkish national agency for basic research (TUBITAK grant no. 133F344).

* dora@eik.bme.hu

- [1] J. Dziarmaga, Adv. Phys. **59**, 1063 (2010).
- [2] A. Polkovnikov, K. Sengupta, A. Silva, and M. Vengalattore, Rev. Mod. Phys. **83**, 863 (2011).
- [3] J. Eisert, M. Friesdorf, and C. Gogolin, Nature Physics **11**, 124 (2015).
- [4] I. Bloch, J. Dalibard, and W. Zwerger, Rev. Mod. Phys. **80**, 885 (2008).
- [5] S. R. White, Phys. Rev. Lett. **69**(19), 2863 (1992).
- [6] J. A. Kjäll, M. P. Zaletel, R. S. K. Mong, J. H. Bardarson, and F. Pollmann, Phys. Rev. B **87**, 235106 (2013).
- [7] U. Schollwöck, Annals of Physics **326**, 96 (2011).
- [8] S. R. Manmana, A. Muramatsu, and R. M. Noack, AIP Conf. Proc. **789**, 269 (2005).
- [9] P. R. Zangara, A. D. Dente, E. J. Torres-Herrera, H. M. Pastawski, A. Iucci, and L. F. Santos, Phys. Rev. E **88**, 032913 (2013).
- [10] A. Daley, C. Kollath, U. Schollwöck, and G. Vidal, J. Stat. Mech.: Theory Exp. (2004), P04005.
- [11] M. P. Zaletel, R. S. K. Mong, C. Karrasch, J. E. Moore, and F. Pollmann, Phys. Rev. B **91**, 165112 (2015).
- [12] S. A. Hamerla and G. S. Uhrig, Phys. Rev. B **89**, 104301 (2014).
- [13] J. Hauschild, F. Pollmann, and F. Heidrich-Meisner, arXiv:1509.00696.
- [14] F. Goth and F. F. Assaad, Phys. Rev. B **85**, 085129 (2012).
- [15] K. Yosida, Phys. Rev. **147**, 223 (1966).
- [16] M. C. Gutzwiller, Phys. Rev. Lett. **20**, 159 (1963).
- [17] M. C. Gutzwiller, Phys. Rev. A **137**, 1726 (1965).
- [18] P. Kramer and M. Saraceno, *Geometry of the Time-Dependent Variational Principle in Quantum Mechanics* (Springer-Verlag, Berlin, 1981).
- [19] D. S. Rokhsar and B. G. Kotliar, Phys. Rev. B **44**, 10328 (1991).
- [20] D. Jaksch, V. Venturi, J. I. Cirac, C. J. Williams, and P. Zoller, Phys. Rev. Lett. **89**, 040402 (2002).
- [21] M. Jreissaty, J. Carrasquilla, F. A. Wolf, and M. Rigol, Phys. Rev. A **84**, 043610 (2011).
- [22] G. Carleo, F. Becca, M. Schiró, and M. Fabrizio, Scientific Reports **2**, 243 (2012), 1109.2516.
- [23] G. Carleo, F. Becca, L. Sanchez-Palencia, S. Sorella, and M. Fabrizio, Phys. Rev. A **89**, 031602 (2014).
- [24] K. Ido, T. Ohgoe, and M. Imada, *Time-dependent many-variable variational Monte Carlo method for nonequilibrium strongly correlated electron systems* (2015), arXiv:1507.00274.
- [25] M. Schiró and M. Fabrizio, Phys. Rev. Lett. **105**, 076401 (2010).
- [26] W. Metzner and D. Vollhardt, Phys. Rev. Lett. **62**, 324 (1989).
- [27] D. Baeriswyl, in *Nonlinearity in Condensed Matter*, edited by A. R. Bishop, D. K. Campbell, D. Kumar, and S. E. Trullinger (Springer-Verlag, 1986).
- [28] B. Valenzuela, S. Fratini, and D. Baeriswyl, Phys. Rev. B **68**, 045112 (2003).
- [29] J. Binemann, S. Wasner, E. v. Oelsen, and G. Seibold, Phil. Mag. **95**, 550 (2015).
- [30] G. Grüner, *Density waves in solids* (Addison-Wesley, Reading, 1994).
- [31] S. Trotzky, Y.-A. Chen, A. Flesch, I. P. McCulloch, U. Schollwöck, J. Eisert, and I. Bloch, Nat. Phys. **8**, 325 (2012).
- [32] P. J. Lee, M. Anderlini, B. L. Brown, J. Sebby-Strabley, W. D. Phillips, and J. V. Porto, Phys. Rev. Lett. **99**, 020402 (2007).
- [33] S. Trotzky, P. Cheinet, S. Fölling, M. Feld, U. Schnorrberger, A. M. Rey, A. Polkovnikov, E. A. Demler, M. D. Lukin, and I. Bloch, Science **319**(5861), 295 (2008).
- [34] See EPAPS Document No. XXX for supplementary material providing further technical details.
- [35] M. S. Foster and A. W. W. Ludwig, Phys. Rev. B **77**, 165108 (2008).
- [36] J. de Woul and E. Langmann, J. Stat. Phys. **139**, 1033 (2010).
- [37] P. Barmettler, M. Punk, V. Gritsev, E. Demler, and E. Altman, New J. Phys. **12**, 055017 (2010).

**SUPPLEMENTARY MATERIAL FOR
"QUANTUM QUENCH IN 2D USING THE
VARIATIONAL BAERISWYL WAVEFUNCTION"**

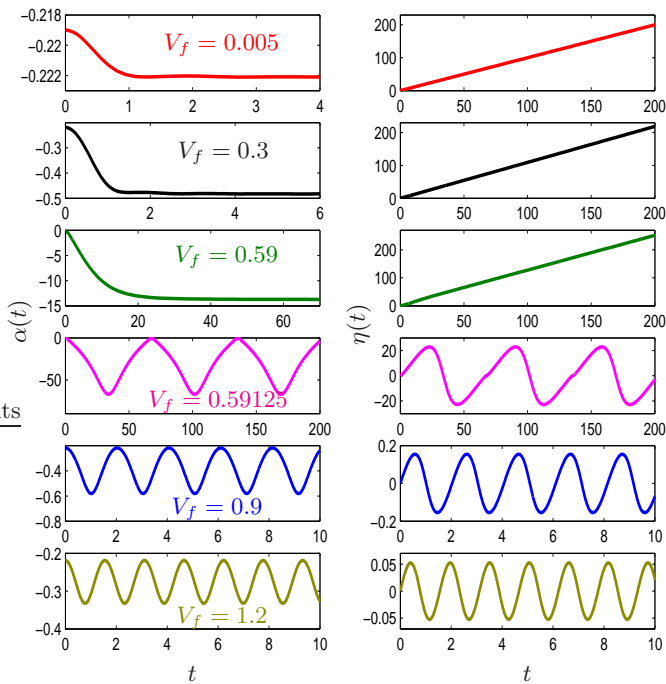


FIG. S1. (Color online) The time dependence of the variational parameters is plotted for $V_i = 1.5$ and several final V_f . The critical interaction strength, separating the steady state and oscillating regimes is around $V_f \approx 0.591$. Note the different horizontal and vertical scales.

ENERGY EXPECTATION VALUE

Due to the structure of the wavefunction, the problem is more tractable when writing the Hamiltonian H in

momentum space as

$$H_{kin} = \sum_{\mathbf{k}} \epsilon(\mathbf{k}) c_{\mathbf{k}}^{\dagger} c_{\mathbf{k}}, \quad (\text{S1})$$

$$H_{int} = -\frac{V}{N} \sum_{\mathbf{k}, \mathbf{k}', \mathbf{q}} \epsilon(\mathbf{q}) c_{\mathbf{k}+\mathbf{q}}^{\dagger} c_{\mathbf{k}} c_{\mathbf{k}'-\mathbf{q}}^{\dagger} c_{\mathbf{k}'}. \quad (\text{S2})$$

The interaction term can be decoupled using Wick's theorem, yielding Eq. (4). The first term in Eq. (4) is the conventional Hartree term, I_1 also comes from the Hartree decoupling by taking the anomalous, $\langle c_{\mathbf{k}}^{\dagger} c_{\mathbf{k}-\mathbf{Q}} \rangle \neq 0$ expectation values into account. The Fock terms give rise to $I_{2,3}$, containing normal, $\langle c_{\mathbf{k}}^{\dagger} c_{\mathbf{k}} \rangle$ and anomalous expectation values, respectively. Due to the rotational symmetry of the square lattice, the x and y directions are completely equivalent to each other, hence the $\cos(k_x a)$ factor in $I_{2,3}$, coming from the \mathbf{q} dependence of the interaction, together with the appropriate combinatorial factors, gives the total variational energy. While the interaction term is even in the variational parameters, the kinetic energy is odd in α and independent of η , therefore their balance determines the optimal variational parameter.

TIME DEPENDENCE OF THE VARIATIONAL PARAMETERS

The numerical solution of Eqs. (9) yield the time-dependent variational parameters, whose behaviour is plotted in Fig. S1. In the steady state regime, the $\eta(t)$ keeps on increasing linearly with time, while $\alpha(t)$ reaches a time independent steady state value. However, the relaxation time required to reach this increases with increasing V_f . At a critical final interaction strength, the solution changes abruptly and both parameters exhibit periodic oscillations. The oscillation frequency increases sharply with V_f , and contain higher harmonics as well close to the critical interaction strength. With increasing V_f , however, a single frequency describes more and more reliably the data.